Molecular Cell
Article

The Conformational Dynamics of the Mitochondrial Hsp70 Chaperone

Koyeli Mapa,[1,2] Martin Sikor,[2,3,4] Volodymyr Kudryavtsev,[2,3,4] Karin Waegemann,[1,2] Stanislav Kalinin,[5] Claus A.M. Seidel,[5] Walter Neupert,[1,2,6] Don C. Lamb,[2,3,4,7,*] and Dejana Mokranjac[1,2,*]
[1]Institute for Physiological Chemistry
[2]Munich Center for Integrated Protein Science (CiPSM)
[3]Physical Chemistry, Department of Chemistry
[4]Center for Nanoscience
LMU München, 81377 Munich, Germany
[5]Molecular Physical Chemistry, Institute of Physical Chemistry II, Building 26.32.02, Heinrich-Heine-University Düsseldorf, Universitätsstrasse 1, 40225 Düsseldorf, Germany
[6]Max Planck Institute of Biochemistry, Am Klopferspitz 18, 82152 Martinsried, Germany
[7]Department of Physics, University of Illinois, Urbana-Champaign, 1110 West Green Street, Urbana, IL 61801, USA
*Correspondence: don.lamb@cup.uni-muenchen.de (D.C.L.), dejana.mokranjac@med.uni-muenchen.de (D.M.)
DOI 10.1016/j.molcel.2010.03.010

SUMMARY

Heat shock proteins 70 (Hsp70) represent a ubiquitous and conserved family of molecular chaperones involved in a plethora of cellular processes. The dynamics of their ATP hydrolysis-driven and cochaperone-regulated conformational cycle are poorly understood. We used fluorescence spectroscopy to analyze, in real time and at single-molecule resolution, the effects of nucleotides and cochaperones on the conformation of Ssc1, a mitochondrial member of the family. We report that the conformation of its ADP state is unexpectedly heterogeneous, in contrast to a uniform ATP state. Substrates are actively involved in determining the conformation of Ssc1. The J protein Mdj1 does not interact transiently with the chaperone, as generally believed, but rather is released slowly upon ATP hydrolysis. Analysis of the major bacterial Hsp70 revealed important differences between highly homologous members of the family, possibly explaining tuning of Hsp70 chaperones to meet specific functions in different organisms and cellular compartments.

INTRODUCTION

Heat shock proteins 70 (Hsp70s) are a highly conserved and ubiquitous class of molecular chaperones. They are involved in a number of processes, including folding of newly synthesized proteins, prevention of protein aggregation, remodeling of protein complexes, and transport of proteins across membranes. These functions depend on the ability of Hsp70 chaperones to bind to and release substrates in an ATP-regulated cycle. Hsp70s transiently bind to exposed hydrophobic regions of unfolded proteins via their substrate-binding domain (SBD). Binding of ATP to the N-terminal nucleotide-binding domain (NBD) induces conformational changes in the SBD that open the substrate-binding pocket and its helical lid. Substrates and J proteins stimulate the hydrolysis of ATP, closing the SBD and trapping the substrate. Nucleotide exchange factors (NEFs) then distort the NBD, which facilitates the release of ADP and the binding of ATP, thereby allowing a new cycle to begin (Bukau et al., 2006; Frydman, 2001; Genevaux et al., 2007; Mayer and Bukau, 2005; Saibil, 2008; Young et al., 2004; Woo et al., 2009). Recently determined high-resolution structures of the full-length Hsp70 proteins and their Hsp110 relatives provided the first insights into the conformations of the end states (Chang et al., 2008; Jiang et al., 2005; Liu and Hendrickson, 2007). However, we are only beginning to understand the dynamics of the chaperone process.

An interesting member of the Hsp70 family is mitochondrial Hsp70 (mtHsp70), which resides in the mitochondrial matrix and is essential for cell viability (Craig et al., 1987; Yoneda et al., 2004). Like other Hsp70 chaperones, it cycles between ATP and ADP states (Horst et al., 1997; Neupert and Brunner, 2002). MtHsp70 uses this cycling to, in cooperation with the J protein Mdj1 and a NEF Mge1, support folding of proteins and prevent their aggregation, like the majority of other Hsp70s (Horst et al., 1997; Kang et al., 1990; Rowley et al., 1994; Westermann et al., 1996). In addition, in cooperation with Mge1 and the J protein Jac1, mtHsp70 plays an important role in the biogenesis of Fe-S clusters (Craig and Marszalek, 2002). Finally, as part of the TIM23 complex, it functions as a molecular motor to drive translocation of proteins across the mitochondrial inner membrane (Endo et al., 2003; Koehler, 2004; Neupert and Brunner, 2002; Neupert and Herrmann, 2007; Rehling et al., 2004). In the TIM23 complex, mtHsp70 is recruited to the matrix side of the translocation channel by Tim44. There, its function is assisted and regulated by a complex that consists of the J protein, Tim14, and the J-like protein, Tim16 (Bolender et al., 2008; Craig et al., 2006; Mokranjac et al., 2006). A specialized chaperone, Hep1, is required to maintain the structure and function of mtHsp70 (Sichting et al., 2005). Recently, mtHsp70 has also been implicated in neurodegenerative disorders and cancerogenesis (Deocaris et al., 2009). While the mitochondria of higher eukaryotes contain only one member of the Hsp70 chaperone family, which fulfills all the functions described above (Schilke et al., 2006), three members of the family are present in yeast

mitochondria (Voos and Röttgers, 2002). The major one, known as Ssc1, mediates folding of proteins and is part of the TIM23 complex, whereas the second member, Ssq1, is involved in the biogenesis of Fe-S clusters. The function of the third one, Ecm10, remains enigmatic (Baumann et al., 2000).

The closest nonmitochondrial homolog of Ssc1 is DnaK, the major bacterial Hsp70 chaperone and a paradigm for Hsp70 research (Genevaux et al., 2007). Even though they share over 50% sequence identity, yeast Ssc1 and DnaK from *Escherichia coli* cannot substitute for each other, neither in bacteria nor in yeast mitochondria (Deloche et al., 1997; Moro et al., 2002). In contrast, the NEFs, Mge1 and its bacterial counterpart, GrpE, as well as the J proteins, Mdj1 from yeast and bacterial DnaJ, can function in both organisms, at least to a certain extent (Deloche et al., 1997; Lisse and Schwarz, 2000). Similar complementation trials between species or between different subcellular compartments of the same organism revealed a surprising degree of specificity of Hsp70 chaperone systems not necessarily expected from the high level of primary sequence conservation among proteins, suggesting evolutionary adaptations of the Hsp70 proteins for specific cellular functions (Brodsky, 1996; Genevaux et al., 2007; Hennessy et al., 2005; Walsh et al., 2004).

In view of the importance of Ssc1, its involvement in a number of essential processes, and the unusually high number of proteins with which it interacts, we set out to analyze its conformational dynamics. To this end, we have developed and applied two Förster Resonance Energy Transfer (FRET)-based sensors in ensemble and single-molecule measurements to investigate the effects of nucleotides and interacting proteins on the relative movement of the two domains of Ssc1 and the opening of the SBD. The single-molecule studies offer the advantage that information regarding the heterogeneity of the sample can be derived from the width of the distribution of FRET efficiencies. Furthermore, subpopulations that are potentially present but hidden in ensemble measurements can be directly observed. Our data demonstrate that the ADP state of Ssc1 is unexpectedly heterogeneous in respect both to domain-domain interaction as well as to the extent to which the lid of SBD is open. In contrast, the interdomain interactions and conformation of the SBD are much more narrowly distributed in the ATP state. We also show that substrates are actively involved in the conformational cycle of Ssc1 and are required for closure of the SBD and full undocking of the domains. Using real-time ensemble FRET measurements, the kinetics of conformational changes during an Hsp70 cycle were monitored. Furthermore, we show that the J protein Mdj1 is released from Ssc1 upon hydrolysis of ATP on the minute timescale. Finally, when similar FRET-based sensors were applied to follow the nucleotide-induced conformational changes of DnaK, important differences between the closely related chaperones were observed, potentially explaining adaptations of Hsp70 proteins to meet specific cellular demands.

RESULTS

A FRET-Based Assay to Analyze the Conformation of Ssc1 in the ATP and ADP States

Residues potentially suitable for the FRET-based analysis of Ssc1 in the absence of any structural information on the complete protein or its domains were identified using the X-ray structure of the SBD of DnaK with bound substrate (Zhu et al., 1996) and that of the ATP form of Sse1, a Hsp110 chaperone that is structurally related to Hsp70s (Liu and Hendrickson, 2007), as described in the Experimental Procedures. The first FRET-based sensor, referred to as the (341,448) sensor, was designed to investigate the NBD-SBD interaction and contained cysteine residues introduced at positions 341 and 448 in the NBD and the SBD, respectively (Figure 1A). The second sensor, referred to as the (448,590) sensor, was used to follow conformational changes of the SBD. It contained cysteine residues at positions 448 and 590, located in the base and the lid, respectively, of SBD. Introduction of cysteine residues at these positions had no effect on the functionality of Ssc1 in vivo (Figure S1A). Labeling of cysteine residues in these constructs with Atto532 maleimide (donor, D) and Atto647N maleimide (acceptor, A) did not affect the basal ATPase activity of Ssc1 nor its stimulation by cochaperones (Figure S1B). Also, anisotropy measurements showed that the fluorophores attached to Ssc1 were free to rotate, ensuring that the orientation of the fluorophores did not significantly influence the detected FRET signal (Table S1). In addition, the anisotropies were not affected by addition of nucleotides, cochaperones, and substrates (Figures S1–S3 and Tables S1, S2, and S4), demonstrating that any measured changes in FRET efficiency would reflect real differences in the conformation of the protein and not artifacts caused by quenching or orientation of the fluorophores.

To test these FRET-based sensors, we first examined the fluorescence spectra upon excitation of donor fluorophore in the presence of either ATP or ADP. The FRET signal in the ensemble measurements was characterized using the ratio of the acceptor fluorescence intensity to the donor fluorescence intensity upon excitation of the donor fluorophore, hereafter referred to as the acceptor-to-donor ratio (AD_R; $AD_R = IP_A/IP_D$, where IP refers to the peak intensity of the acceptor or donor channel). The spectrum obtained for the (341,448) sensor revealed a higher AD_R in the presence of ATP than in the presence of ADP (Figure 1B). This suggests that the two domains of Ssc1 are closer to each other in the presence of ATP than in the presence of ADP. In contrast, the fluorescence spectrum obtained for the (448,590) sensor revealed a higher AD_R in the presence of ADP than in ATP (Figure 1C). The SBD appears to be open in the ATP state and more closed in the ADP state. Upon denaturation of Ssc1, no FRET signal was observed (i.e., the AD_R was essentially 0) (Figure S1C), providing further support that the observed FRET signals are due to the change in Ssc1 conformation. Thus, two sensors can be used to monitor the conformational changes between the ATP and ADP states of Ssc1.

To gain more detailed information regarding the conformations of Ssc1 under different nucleotide conditions, single-pair FRET (spFRET) experiments were performed (Figures 1D–1G). The data were collected using pulsed interleaved excitation (PIE) (Kapanidis et al., 2004; Müller et al., 2005; Sharma et al., 2008) to ensure that only molecules with photoactive donor and acceptor fluorophores were incorporated into the spFRET histograms. We analyzed the single-molecule data using the probability distribution analysis (PDA) (Antonik et al., 2006; Kalinin et al., 2007, 2008), which enables rigorous determination of

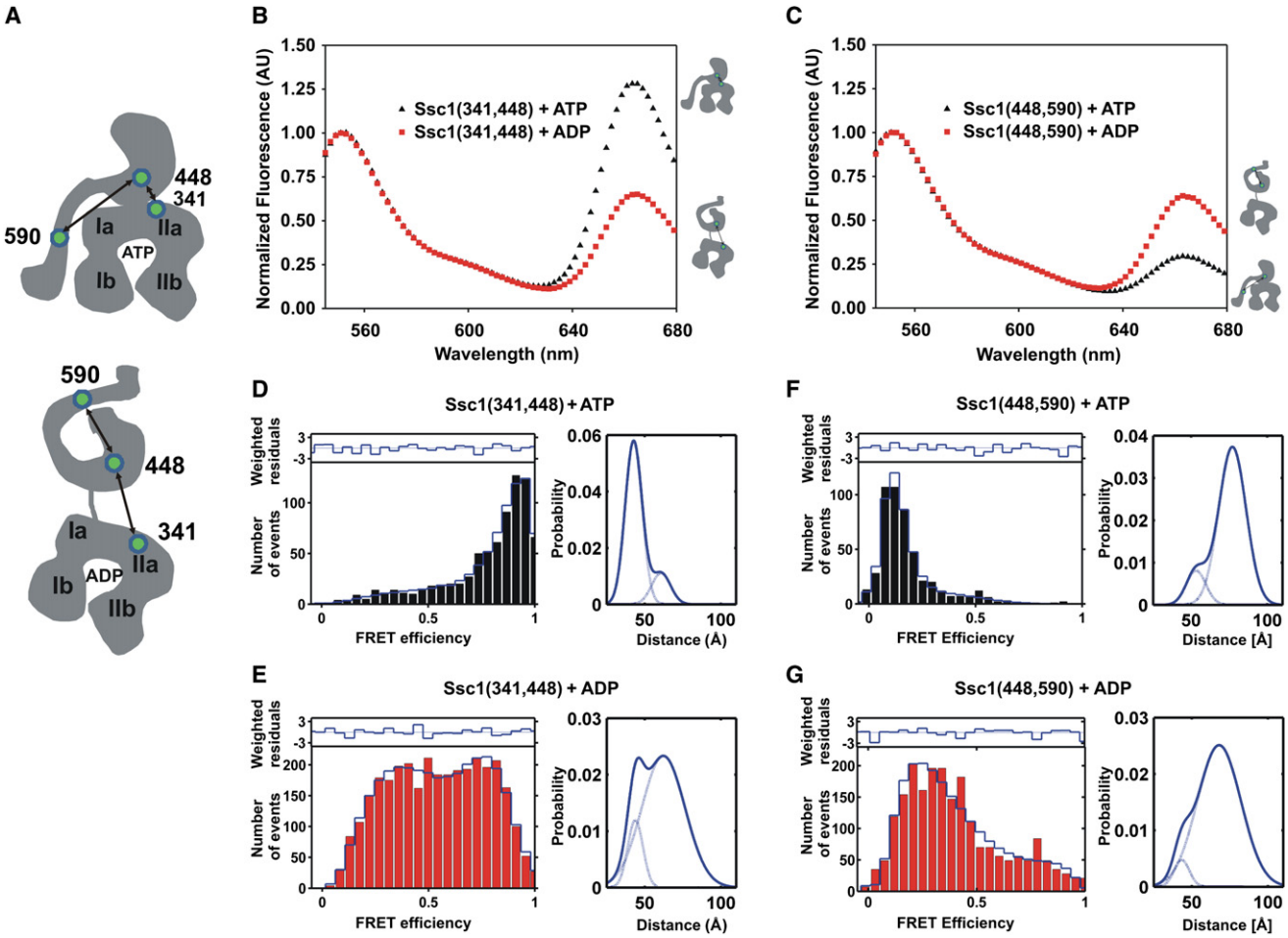

Figure 1. Conformational Changes of Ssc1 in Different Nucleotide States Probed by Ensemble and SpFRET Measurements

(A) Schematic representation of Ssc1 in ATP (upper panel) and ADP (lower panel) states indicating the positions of engineered cysteines. Arrows indicate the distance vectors monitored by intramolecular FRET measurements to follow the conformational changes.

(B) To monitor the changes in interdomain distance of Ssc1, double-labeled Ssc1 (341,448) was preincubated with either 2 mM ATP (black curve) or 2 mM ADP (red curve), and the fluorescence spectra were recorded after exciting the donor fluorophore at 530 nm. The fluorescence at 550 nm was normalized to one.

(C) To monitor the changes in the conformation of the SBD, double-labeled Ssc1 (448,590) was analyzed as described in (B).

(D and E) SpFRET measurements with weighted residuals of double-labeled Ssc1 (341,448) in the ATP (D, left panel) and ADP states (E, left panel) and corresponding distance distributions determined using PDA (right panels).

(F and G) Double-labeled Ssc1 (448,590) was analyzed as in (D) and (E). See also Figure S1 and Table S1.

the number of species present and the homogeneity of the individual states for single-molecule FRET measurements with overlapping populations, as explained in Supplemental Experimental Procedures. The single-molecule histograms of FRET efficiencies (f_e) for the (341,448) sensor showed a narrow distribution peaking at $f_e = 0.89$ in the ATP state (Figure 1D, left panel) and a very broad distribution in the ADP state (Figure 1E, left panel) with a peak shifted to lower FRET efficiencies. At least two distributed subpopulations were required to describe each nucleotide-bound state. However, in both cases, one population was very dominant and comprised at least 80% of molecules, suggesting distinct relative orientations of the domains in ATP and ADP states (Figures 1D–1G, right panels; see also Table 1 for more details). The population of the minor species varied with sample preparations and could be due to the biochemical impurities within the sample (e.g., hydrolyzed ATP, inactive protein). Alternatively, the protein may exist in two conformations, and binding of the different nucleotides alters the equilibrium between these conformations. The dominant population (80%) in the ATP state had an average donor-acceptor separation of ~42 Å and was relatively narrow (the standard deviation [SD] of the Gaussian distribution was 5.5 Å) (Figure 1D, right panel). In contrast, in the dominant subpopulation (83%) of the ADP state, the average donor-acceptor separation increased to ~62 Å and was very broad (SD = 14 Å) (Figure 1E, right panel). Thus, the hydrolysis of ATP to ADP not only separated the two domains of Ssc1 but also allowed for more conformational variability in interactions between the NBD and SBD.

Analysis of the SBD conformation with the (448,590) sensor also required at least two subpopulations to describe each spFRET histogram, with again one predominant population in

Table 1. Photon Distribution Analysis of SpFRET Distributions

	Major Subpopulation			Minor Subpopulation			D-only	
	%	d [Å]	SD [Å]	%	d [Å]	SD [Å]	%	Reduced χ^2
Ssc1(341,448)/ATP	80	42.7	5.5	17	60.7	6.2	3	1.04
Ssc1(341,448)/ADP	83	62.2	14.2	15	43.8	5.0	2	1.72
Ssc1(341,448)/ATP + Mdj1	85	59.5	11.8	13	47.3	2.3	2	1.30
Ssc1(341,448)/ATP + Mdj1/P5	100	75.3	11.5	-	-	-	0	1.57
Ssc1(448,590)/ATP	84	77.1	9.0	13	53.2	6.4	3	0.65
Ssc1(448,590)/ADP	90	67.9	14.3	10	43.3	5.0	0.0	1.00
Ssc1(448,590)/ATP + Mdj1	95	67.7	10.3	-	-	-	5[a]	2.01[b]
Ssc1(448,590)/ATP + Mdj1/P5	84	51.8	4.3	15	63.9	8.9	1	0.92
DnaK(318,425)/ATP	84	47.3	3.0	15	67.6	15.9	1	1.51
DnaK(318,425)/ADP	89	84.2	8.6	8	53.2	4.6	3	1.15
DnaK(458,536)/ATP	100	87.4	9.9	-	-	-	0	1.87
DnaK(458,536)/ADP	61	78.7	15.3	30	58.8	3.3	9[a]	1.63

The results from a PDA analysis where the ADP, ATP, and ATP + Mdj1 samples were fit with either one or two Gaussian distributions in donor-acceptor separation with peak separation distance (d) and width (SD). The individual bursts were divided into time bins of 2 ms, and the histogram of the logarithm of the ratio of green to red fluorescence intensities for the individual bins was determined and modeled with PDA. In all measurements, a small fraction of a zero-FRET or donor-only species was present.

[a] As seen for most experiments, a small zero-FRET or donor-only species was present in the data (0%–3%) even with the use of PIE. This could be due to the presence of a transient-dark state or photobleached acceptor for time windows within a burst. However, samples with a higher zero-FRET contribution indicate the presence of an additional subpopulation with donor-acceptor separation larger than ~10 nm that is no longer detectable with FRET.

[b] The distribution of FRET efficiencies of the Ssc1(448,590)/ATP + Mdj1 was fit with a single Gaussian model, which gives a distribution similar to the main population of Ssc1(448,590)/ADP. The data suggest that more subpopulations are present in the sample, but the details could not be uniquely extracted from the data set.

each nucleotide state. In the ATP state, a dominant f_e peak (84%) at 0.20 (corresponding to a distance of ~77 Å) was observed, demonstrating that the SBD is open when ATP is bound (Figure 1F). The width of this distribution was ~9 Å. In the ADP state, the spFRET histogram was very broad and shifted to higher FRET efficiencies (Figure 1G, left panel). The major population (90%) had a donor-acceptor separation of 68 Å and a width of 14 Å. Thus, the single-molecule data show a more closed and less well-defined population of the SBD in the ADP state than in the ATP state of the chaperone.

The broader distributions obtained for both sensors in the ADP state of the chaperone suggest that the protein is more flexible in this conformation. To support this notion, we analyzed the FRET efficiencies of individual bursts, E, as a function of the donor fluorescence lifetime, $\langle\tau\rangle_{avg}$, averaged over the burst. This method, recently described in Gansen et al., 2009, is discussed in detail in the Supplemental Information. Briefly, an approximately linear relationship between E and $\langle\tau\rangle_{avg}$ is expected for a static sample. However, when a molecule fluctuates between different conformations during a burst, the linear relationship is no longer observable. This analysis supports dynamic fluctuations occurring within the burst, which has an average duration of ~5 ms, between conformations for the (341,448) sensor in the ADP state (Figure S1E). In the ATP state of the (341,448) sensor, the main population showed a well-defined static population with high FRET efficiency (Figure S1D). Dynamics are detected in a minor population, which most likely represents a minor ADP population in the sample. In contrast, the ATP and ADP states of the (448,590) sensor gave no indication of dynamics on the 5 ms timescale (Figures S1F and S1G).

Taken together, these data demonstrate that the conformation of the ATP state of Ssc1 is fairly homogeneous with an open, though still flexible, SBD, and the two domains are docked. In contrast, the ADP state of Ssc1 appears to be rather broadly distributed, both in respect to the NBD-SBD interaction and the conformation of the lid. At least for the (341,448) sensor, the broad distribution suggests flexibility in the NBD-SBD interactions.

Influence of Mdj1 and Substrate on the Conformation of Ssc1

To investigate the conformation of Ssc1 during the folding cycle in the mitochondrial matrix, the J protein partner of Ssc1, Mdj1, alone or together with the substrate peptide P5, was added to Ssc1 in the presence of ATP. The data obtained with both sensors in the presence of Mdj1 were similar to that observed in the presence of ADP. This was seen in the ensemble measurements (Figures 2A and 2D) as well as in the FRET histograms (Figure 2B) and graphs of dynamics analysis (Figures S2A and S2C) of the single-molecule data. This demonstrates that Mdj1 stimulates the ATPase activity of Ssc1 and converts the ATP form of the chaperone into the ADP one. In contrast, dramatic differences in the FRET signal were observed in the presence of Mdj1 and the substrate P5 (Figures 2A, 2C, 2D, and 2F). The (341,448) sensor showed a lower AD_R than in the presence of ADP or only Mdj1 in the ensemble measurements (Figure 2A). In the single-molecule measurements, a shift to a single peak with a lower FRET efficiency was observed (Figure 2C, left panel). The average distance between the fluorophores increased from ~62 Å in the ADP state to ~75 Å in the

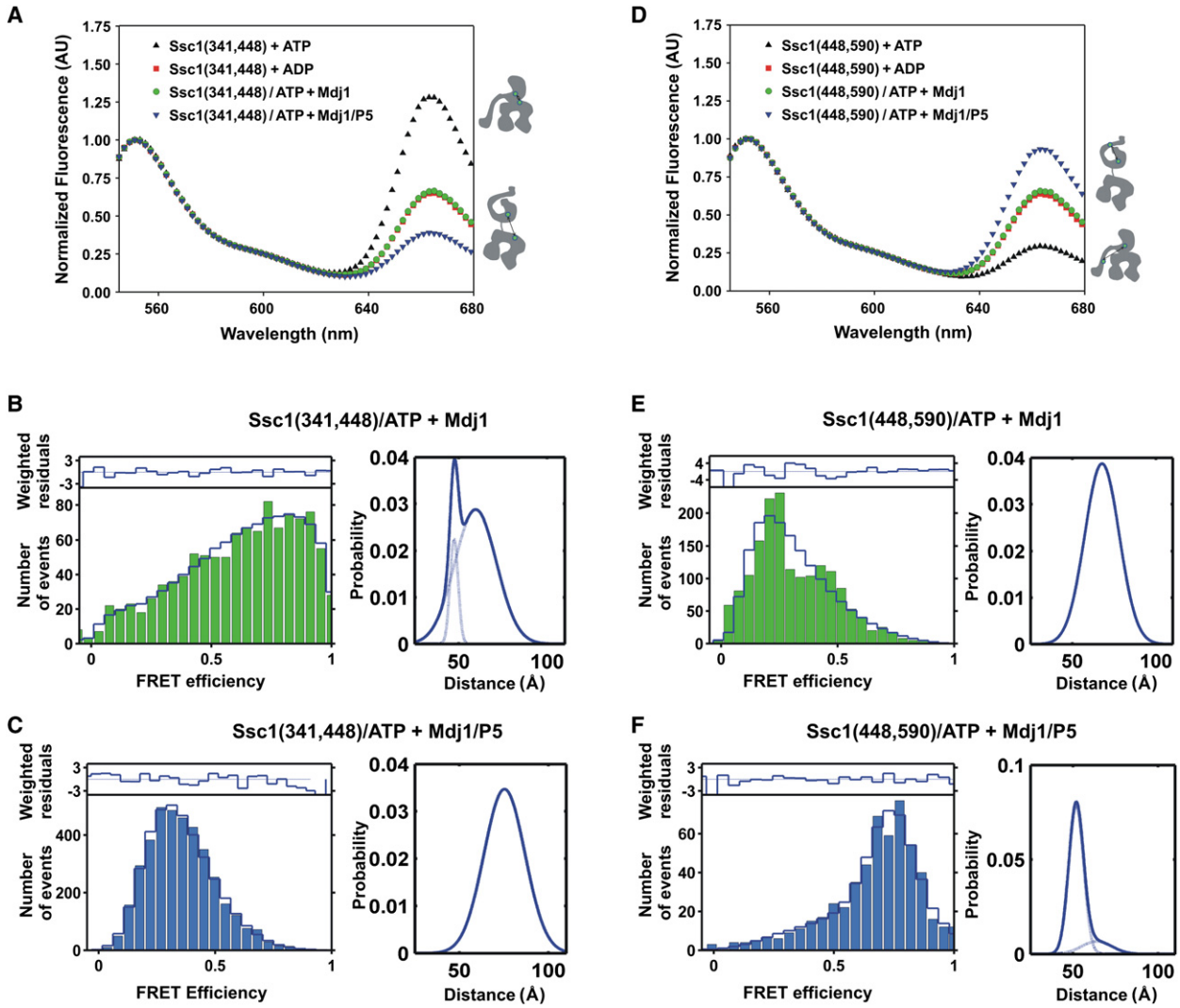

Figure 2. Effects of Mdj1 and Substrate Peptide P5 on the Conformation of Ssc1 Determined by Ensemble and SpFRET Measurements

(A–C) Mdj1, alone or together with P5 peptide, was added to the (341,448) sensor, as described in the Experimental Procedures. Samples were analyzed by ensemble (A) and spFRET measurements with Mdj1 (B) and with Mdj1 and P5 (C).

(D–F) Same as (A)–(C), except that the (448,590) sensor was analyzed. Fluorescence at 550 nm was normalized to one in (A) and (D). Weighted residuals are shown in the upper panels of the single-molecule experiments, and the corresponding distance distributions determined using PDA are displayed in the right panels. See also Figure S2 and Table S2.

presence of substrate (Figure 2C, right panel, and Table 1), indicating that the substrate is required for full undocking of the two domains of Ssc1. On the other hand, in the ensemble measurements, the (448,590) sensor revealed a higher AD_R in the presence of substrate as compared to ADP or Mdj1 only (Figure 2D). In the single-molecule measurements, a dominant (84%) FRET peak corresponding to an average donor-acceptor separation of 52 Å and a width of 4.3 Å (Figure 2F, right panel, and Table 1) was observed, implying that protein is in a well-defined conformation. Thus, the lid of Ssc1 shows a well-defined, closed conformation only in the presence of the substrate. Taken together, these data demonstrate that substrates have an active role in the conformational dynamics of Ssc1.

Real-Time Measurements of the Ssc1 Cycle

Using the FRET sensors discussed above, we followed the conformational changes of Ssc1 in real time by monitoring the changes in the AD_R (Figure 3). Domain undocking due to the spontaneous hydrolysis of ATP by Ssc1 occurred with the slowest kinetics and was accelerated in the presence of the substrate peptide P5 and even further by Mdj1 (Figure 3A). Consistent with the observed distribution of conformations, the reaction kinetics could be well fit to a stretched exponential, but for the sake of comparison, we approximated the rates as single exponentials. The reaction rates were similar to the ATP hydrolysis rates under the same conditions (Table S3), suggesting that hydrolysis of ATP and domain undocking occur

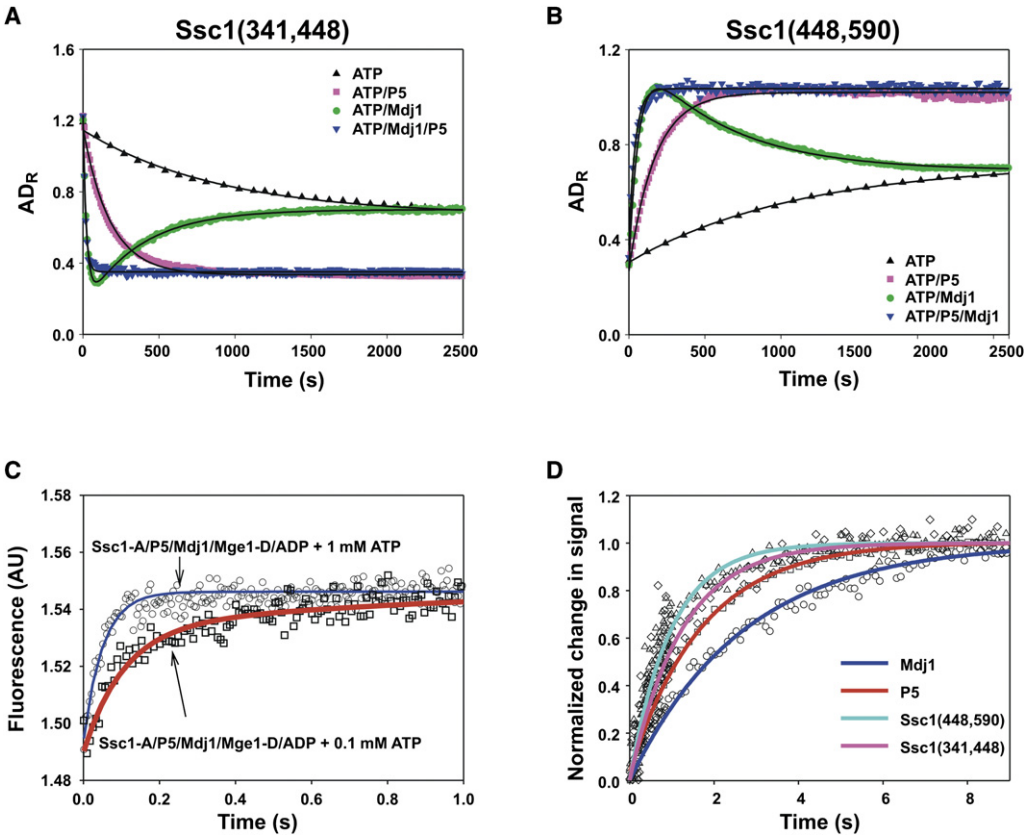

Figure 3. Kinetics of the Ssc1 Chaperone Cycle

(A and B) The kinetic traces of domain undocking analyzed using the (341,448) sensor (A) and lid closing analyzed using the (448,590) sensor (B) were obtained by monitoring the change in AD_R under single-turnover conditions as described in Supplemental Experimental Procedures. The change in AD_R was monitored during unstimulated hydrolysis of ATP by Ssc1 or after addition of Mdj1 (4 μM) and/or P5 (50 μM).

(C) A complex consisting of acceptor-labeled Ssc1 (Ssc1-A), donor-labeled Mge1 (Mge1-D), P5, Mdj1, and ADP was mixed with 0.1 mM (blue curve) or 1 mM ATP (red curve) in a stopped-flow device in presence of 1 μM unlabelled Mge1, and the dissociation kinetics of Mge1 were monitored as the recovery of donor fluorescence.

(D) Kinetics of conformational changes of Ssc1 and dissociation kinetics of Mdj1 and P5 from Ssc1/ADP/Mdj1/P5/Mge1 complex upon binding of ATP. Kinetics of Mdj1 dissociation (blue curve) were monitored by recovery of donor fluorescence of donor-labeled Mdj1 after mixing Ssc1/ADP/Mdj1/P5/Mge1 complex, containing acceptor-labeled Ssc1 and donor-labeled Mdj1, with 2 mM ATP in the presence of unlabeled Mdj1. Dissociation of P5 (red curve) was monitored as for Mdj1, with the difference that P5 was donor-labeled and unlabeled P5 was present in excess. Kinetics of conformational changes of Ssc1 were monitored as changes in the AD_R after mixing Ssc1/ADP/Mdj1/P5/Mge1 complex containing double-labeled Ssc1 with 2 mM ATP in a stopped-flow mixing device (the [341,448] sensor, pink curve; the [448,590] sensor, cyan curve). To provide visual comparison of different rates, normalized changes in the signals are plotted. See also Table S3.

essentially simultaneously. Under the same conditions, closing of the SBD could be followed by the increase of the acceptor fluorescence in the (448,590) sensor (Figure 3B). Lid closing in the presence of Mdj1 and peptide occurred with slightly slower kinetics as compared to hydrolysis of ATP (Table S3), indicating that the domain undocking occurs on the same timescale and may even precede closure of the lid. Interestingly, the kinetics observed for both the domain-undocking and the lid-closing reactions in the presence of Mdj1 without substrate revealed an unexpected behavior (Figure 3). Mdj1 alone was able to undock the two domains and close the lid but could not sustain this conformation. After initial domain undocking and lid closure, the conformation of Ssc1 slowly reverted to that of the ADP-only state.

The productive folding of substrates requires their release from the chaperone. This is achieved by release of ADP and rebinding of ATP to the chaperone in a reaction stimulated by NEFs, Mge1 in the case of mitochondria. We analyzed the kinetics of these steps using FRET-based assays in a stopped-flow apparatus. Mge1 bound to Ssc1 in the absence of ATP (data not shown) and was released upon addition of ATP (Figure 3C). The rate of Mge1 release was dependent on the ATP concentration, indicating that ATP binding is the rate-limiting step of Mge1 release. Subsequent conformational changes of Ssc1 were analyzed by following the changes of AD_R in the (341,448) and (448,590) sensors, and the release of Mdj1 and P5 peptide was followed by the recovery of the donor fluorescence as described in the Supplemental Experimental

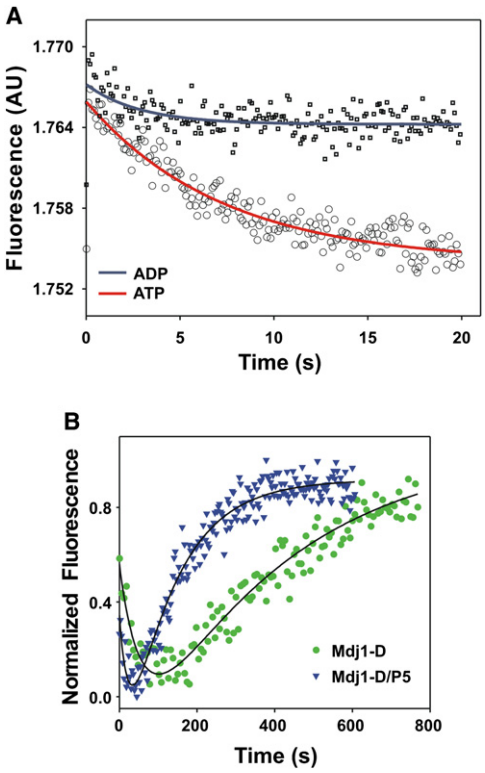

Figure 4. Interaction of Mdj1 with Ssc1

(A) Donor-labeled Mdj1 was mixed with acceptor-labeled Ssc1 in the presence of 2 mM ATP (red curve) or 2 mM ADP (blue curve) in a stopped-flow device, and the donor fluorescence was monitored over time.

(B) Interaction of donor-labeled Mdj1 (Mdj1-D), in the absence (green curve) or presence (blue curve) of substrate (50 μM P5, premixed with Mdj1), with acceptor-labeled Ssc1 was monitored upon manual mixing under single-turnover conditions as described in Supplemental Experimental Procedures. Since Mdj1-D does not rebind to the ADP state of Ssc1 formed upon ATP hydrolysis, the off-rate could be observed even in the absence of nonlabeled Mdj1.

Procedures. Upon binding of ATP, docking of the domains and opening of the lid occurred with very similar kinetics, followed by the release of the substrate and Mdj1 (Figure 3D). Interestingly, whereas the release of Mge1 occurred on the millisecond timescale, the subsequent conformational changes of Ssc1 happened on the second timescale.

Interaction of Ssc1 with Mdj1

The unexpected kinetics of conformational changes of Ssc1 observed in the presence of Mdj1 (Figures 3A and 3B) prompted us to investigate their interaction in more detail. Therefore, we developed a FRET-based assay to directly visualize their interaction. To this end, Mdj1 was labeled with Alexa 594 as the donor fluorophore and Ssc1 with Atto647N as the acceptor fluorophore. Upon mixing of the labeled Mdj1 and Ssc1, a decrease in donor signal was observed in the presence of ATP, but no significant change was observed in the presence of ADP (Figure 4A), indicating that Mdj1 interacts with Ssc1 in its ATP form but not in the ADP form. In the presence of 200 nM Mdj1 and 500 nM Ssc1, binding occurred within ~15 s (Figure 4A). Upon longer recordings, Mdj1 bound to Ssc1 was subsequently released from the chaperone on the minute timescale (Figure 4B). Interestingly, if substrate was present in the reaction, the release of Mdj1 from the chaperone was accelerated by a factor of two (Figure 4B). These results imply that Mdj1 binds quickly to Ssc1 but is released much more slowly. Furthermore, the presence of the substrate has a pronounced effect on Ssc1-Mdj1 interaction.

Analysis of the Conformational Distribution of DnaK by Corresponding FRET-Based Sensors

To understand the differences between Ssc1 and DnaK that underlie the inability of the highly homologous chaperones to substitute for each other, we analyzed the conformational distribution of DnaK in the presence of ATP and ADP. We introduced cysteine residues at the positions in *E. coli* DnaK similar to the ones described above for Ssc1 (Figure 5A). Like in the case of Ssc1, fluorophores attached to DnaK were free to rotate under all conditions analyzed, showing that the FRET signals are due to the real conformational changes of the protein (Figure S3 and Table S4). Ensemble FRET measurements of both sensors obtained in the presence of ATP and of ADP revealed results similar to those obtained for Ssc1, demonstrating that these sensors can be used with Hsp70 chaperones in general (Figures 5B and 5C). At single-molecule resolution, the ATP state of DnaK was well defined, with the two domains docked onto each other (average separation of 47 Å) and an open SBD (87 Å) in the dominant subpopulations, as observed for Ssc1 (Figures 5D and 5E, left panels, and Table 1). In the ADP state of DnaK, its SBD adopted at least two conformations (Figure 5E, right panel), similar to what was observed for Ssc1. However, in contrast to Ssc1, the two domains of DnaK in the ADP state were largely separated (Figure 5D, right panel), and no dynamics were seen on the 5 ms timescale (Figure S3), indicating inherent differences in the behavior of the highly homologous members of the Hsp70 family.

DISCUSSION

In this study, we explored the conformational cycle of Ssc1, a mitochondrial member of the Hsp70 family of chaperones, using ensemble and spFRET. Our data, summarized in Figure 6, demonstrate that the ATP state of Ssc1 is well defined, with an open lid and the NBD and SBD docked. In contrast, the ADP state of Ssc1 is rather heterogeneous, with some contacts between the domains still remaining. Our results on the ATP state of Ssc1 are in agreement with the data obtained earlier with DnaK and other Hsp70 chaperones (Buchberger et al., 1995; Swain et al., 2007). Thus, it seems that the ATP state of Hsp70 chaperones in general has two domains docked onto each other and an open SBD. The distance between the two domains estimated from the spFRET data for the distance between residues 341 and 448 (42 Å) is in good agreement with the distance obtained from the model of Ssc1 structure based on the crystal structure of Sse1 (41 Å). The domain-domain interactions in the ATP state of Hsp70 and of Hsp110 chaperones are therefore indeed very similar. Interestingly, the calculated distance of 77 Å between residues 448 and 590 in the base and the lid of

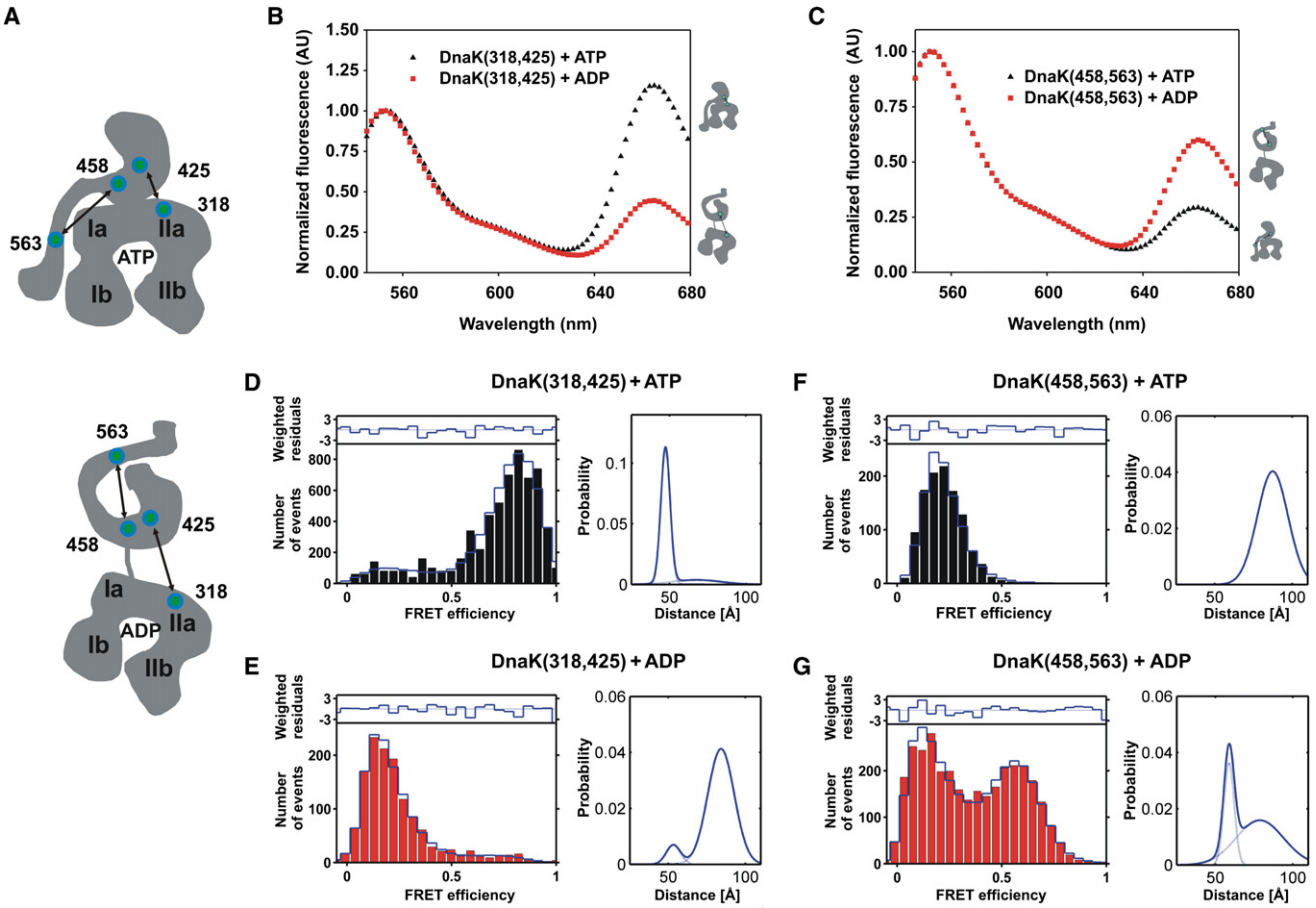

Figure 5. Conformational Changes of DnaK in Different Nucleotide States Probed by Ensemble and Single-Molecule FRET Measurements

(A) Schematic representation of DnaK in ATP (upper panel) and ADP (lower panel) states, indicating the positions of engineered cysteines. Arrows indicate the distance vectors monitored by intramolecular FRET measurements to follow the conformational changes.

(B and C) Fluorescence spectra (with 530 nm excitation) of double-labeled DnaK (318,425) (B) and DnaK (458,563) (C) when preincubated with either 2 mM ATP (black curves) or 2 mM ADP (red curves).

(D and E) Distribution of FRET efficiencies in the ATP (D, left panel) and ADP states (E, left panel) were determined by spFRET measurements of double-labeled DnaK (318,425).

(F and G) Same as (D) and (E), except that the double-labeled DnaK (458,563) was analyzed. Weighted residuals are shown in the upper panels of the single-molecule experiments, and the corresponding distance distributions determined using PDA are displayed in the right panels. See also Figure S3 and Table S4.

SBD of Ssc1 is smaller than the distance obtained from the model (85 Å). This suggests that Hsp70 chaperones cannot open their SBD as widely as Hsp110s and is consistent with the observation that the helices A and B of the SBD of Hsp70s are combined into a single helix in the Hsp110s (Andréasson et al., 2008; Liu and Hendrickson, 2007; Polier et al., 2008; Schuermann et al., 2008). Indeed, a third FRET-based sensor, made to investigate the interaction between the NBD and the lid of SBD in Ssc1, revealed a FRET efficiency far lower than expected from the structure of Sse1 (Liu and Hendrickson, 2007) (K.M. and D.M., unpublished data), supporting the above notion.

In contrast to the ATP state, the ADP state of Ssc1 is more heterogeneous, having broad distributions of distances with respect to both domain-domain interaction as well as the conformation of the SBD. The single-molecule analysis also shows that the ADP state is dynamic, linking the heterogeneity of the distribution to the dynamics of NBD-SBD interaction in Ssc1. Reports present in the literature describing the ADP states of different Hsp70 chaperones are apparently conflicting. Extensive interdomain interactions were suggested for the ADP state of the mammalian Hsc70 (Jiang et al., 2005, 2007). On the other hand, the NBD and SBD of DnaK were found to behave independently in its ADP form (Bertelsen et al., 2009; Swain et al., 2007). Our spFRET analysis of DnaK also suggests that in the ADP state, the two domains are completely undocked, even though the SBD is not closed. Thus, the ADP state of Ssc1 appears more similar to Hsp70s of higher eukaryotes than to DnaK. Taking into account the above notion that the ATP states of all Hsp70 chaperones and their homologs are very similar, it seems that the conformational changes induced by the hydrolysis of ATP in the NBD are conveyed to the SBD in different ways.

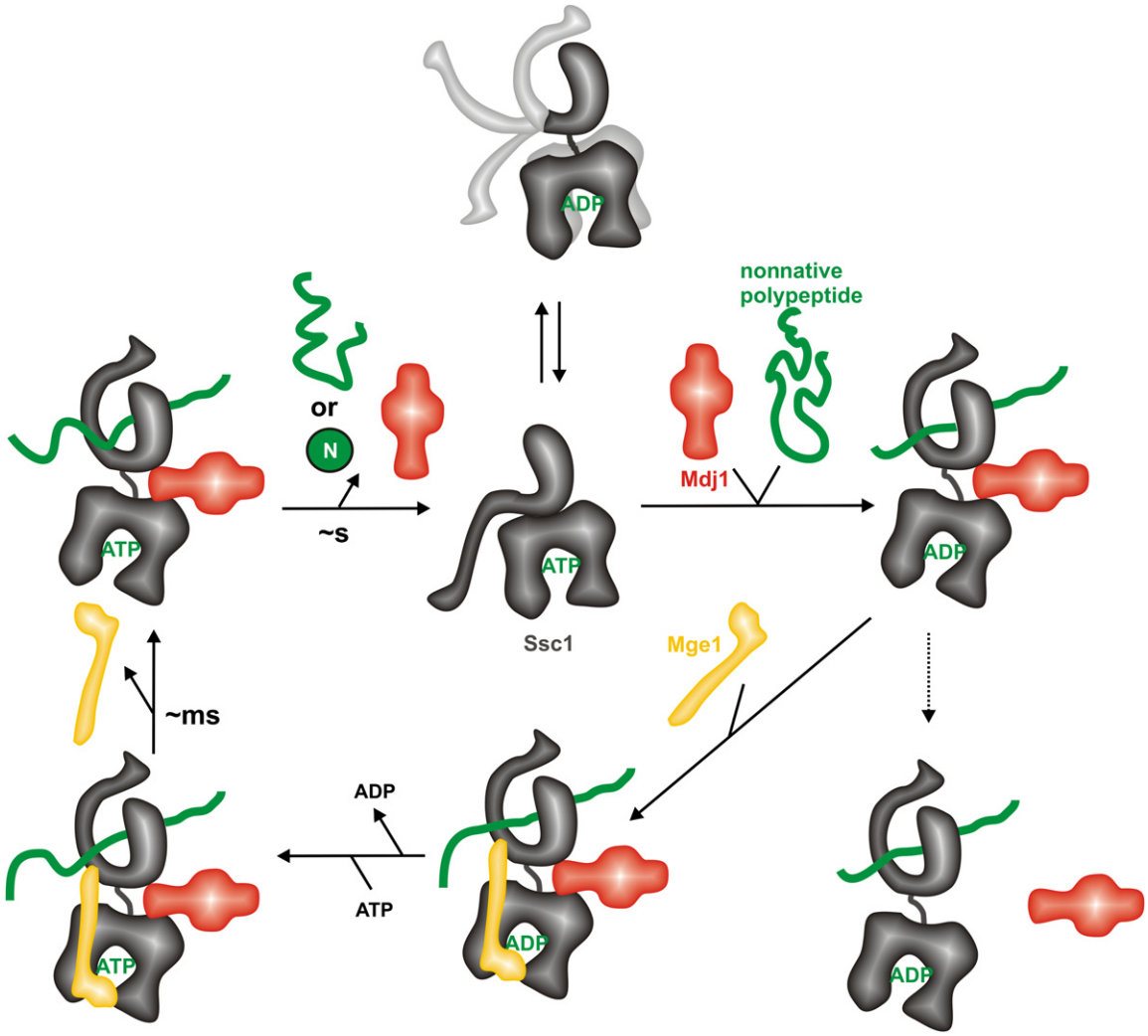

Figure 6. Model of the "Folding Cycle" of Ssc1

In its ATP state, Ssc1 is a compact molecule with an open SBD and the two domains docked. Spontaneous hydrolysis converts the ATP state to the ADP state, which is very heterogeneous in respect both to domain-domain interaction as well as to the extent to which the SBD is opened. The J protein Mdj1 enables binding of a substrate to the ATP state of Ssc1 by stimulating the hydrolysis of ATP. The ADP state of Ssc1 with the bound substrate is characterized by the domains being fully undocked and the SBD closed. In the absence of ATP and NEF Mge1, Mdj1 will be released from this complex with a half-life of ~5 min (dashed arrow). Binding of Mge1 increases the rate of ADP release. In the presence of ATP, Mge1 will be released from the complex within milliseconds, followed by conformational changes of Ssc1, which induce release of Mdj1 and the substrate from the chaperone.

The key elements involved in allosteric regulation, the residues of the recently proposed proline switch (Vogel et al., 2006a), those of the interdomain linker (Swain et al., 2007; Vogel et al., 2006b), and the ones affected by rotation of subdomains of NBD (Bhattacharya et al., 2009), are essentially invariant among a range of Hsp70 chaperones. This implies that the subtle differences in the primary sequence are probably sufficient to produce rather different ADP states of various Hsp70 chaperones, likely reflecting specialization of Hsp70 chaperones for different cellular functions.

The role of substrates in the conformational cycle of Hsp70s has remained unclear largely due to the apparent difficulties in obtaining them in ADP-bound but substrate-free forms (Swain et al., 2006). Our data demonstrate an active role of substrates in determining the conformation of Ssc1. The conformations of the ADP states of Ssc1 in the absence and in the presence of substrate were found to be very different. In both ensemble and spFRET measurements, the presence of the substrate was necessary for full undocking of the NBD and SBD and for lid closure of Ssc1. In contrast, according to our data with DnaK, ADP alone was sufficient to undock the domains even though the SBD was still flexible and binding of the substrate is likely needed for its closure, as well. One possible explanation for the observed differences between Ssc1 and DnaK is the involvement of Ssc1 in the translocation process. Ssc1, most likely in its ATP state, is recruited to the outlet of the translocation channel, where it binds to the incoming polypeptide chain concomitant with hydrolysis of ATP to ADP. Subsequent release of the

polypeptide-bound Ssc1 from the translocase enables the vectorial movement of the polypeptide across the membrane into the mitochondrial matrix. Although the sequence of events during this process still remains largely unclear, it is reasonable to assume that binding of the polypeptide segment to Ssc1 is recognized by the translocase in order to ensure the release of only substrate-bound Ssc1. The increase in interdomain separation upon peptide binding may provide such a signal.

Furthermore, we observed a rather intriguing binding behavior of Mdj1 to Ssc1. As expected, the cochaperone bound to the ATP form of Ssc1 and stimulated ATP hydrolysis. However, Mdj1 remained bound to Ssc1 with a half-life of the complex of ~5 min. This is in agreement with the observation that the Mdj1-Ssc1 complex could be recovered from mitochondria solubilized in the presence of ATP (Horst et al., 1997). Other J proteins, such as DnaJ and Sec63, were proposed to bind very transiently to their Hsp70 partners (Bukau and Horwich, 1998; Jiang et al., 2007). When stable binding was observed with these J proteins, it was because they apparently acted as substrates for the Hsp70s (Misselwitz et al., 1999). In contrast, Mdj1 is not bound to Ssc1 in a substrate-like manner. This binding behavior of Ssc1 to its J protein(s) raises an important issue. In the context of the "folding cycle" of Ssc1 in the mitochondrial matrix, Mdj1 will be released from Ssc1 within 1 s in the presence of Mge1 and ATP, enabling a quick reinitiation of the folding cycle. However, in the context of the Ssc1 cycling during translocation of proteins into mitochondria via the TIM23 complex, such a prolonged association with the membrane-bound J protein, Tim14, would be deleterious, as it would prevent rapid movement of the substrate-bound Ssc1 away from TIM23. Delayed movement of the translocating chain into the matrix would lead to jamming of the translocase and, eventually, cell death. On the other hand, rapid dissociation of the Ssc1-substrate-Tim14 complex by Mge1 and ATP would also be counterproductive, as the substrate would be released at the same time rather than remaining bound to Ssc1 until it has moved into the mitochondrial matrix. How nature has resolved this issue is still not clear, but it is likely that the presence of at least two more proteins directly involved in the "translocation cycle" of Ssc1, Tim44, and Tim16 and their interplay with the components of the translocation channel will be essential in resolving this important issue. Clearly, in the elucidation of the function and dynamics of the Hsp70s, FRET experiments will play an important role in the future.

EXPERIMENTAL PROCEDURES

Cysteine Mutants of Ssc1

Residues of Ssc1 suitable for positioning of the fluorophores were identified by modeling Ssc1 on the structures of the SBD of DnaK (PDB accession number 1 dkx) and of the ATP state of Sse1 (PBD accession number 2qxl) using SWISS-MODEL (http://swissmodel.expasy.org/). The selected amino acids were D341, I448, and D590. According to the sequence alignment made by DNAMAN, these residues correspond to E318, V425, and A564 of *E. coli* DnaK; D315, T427, and D572 of bovine Hsc70; and E319, R435, and K600 of yeast Sse1. The selected amino acids of Ssc1 were mutated to cysteines using QuikChange mutagenesis protocol (Stratagene; Cedar Creek, TX) in the plasmid pETDuet1-Hep1-Ssc1, which allows for expression of soluble and functional Ssc1 in bacteria (Sichting et al., 2005). The plasmid pETDuet1-DnaK, which contained *E. coli DnaK* (a gift from M. Sichting), was used for introduction of cysteines in DnaK with the modification that the endogenous cysteine at position 15 of DnaK was first mutated to alanine and the obtained plasmid subsequently used as template for site-directed mutagenesis. Wild-type Ssc1 does not contain endogenous cysteines.

Proteins

Wild-type or cysteine mutants of Ssc1 were expressed in BL21(DE3) cells as described previously (Sichting et al., 2005). Proteins were purified on a His_6-Mge1 column using a modified protocol for purification of Ssc1 from yeast mitochondria (Weiss et al., 2002). Briefly, the cell lysate, containing mature Ssc1 and His_6-Hep1 in 50 mM Tris-HCl (pH 7.5), 250 mM KCl, 5 mM $MgCl_2$, and 5% glycerol, was loaded on a Ni-NTA-Agarose column to remove His_6-Hep1 prior to binding of Ssc1 to the His_6-Mge1 column. The proteins were stored at −80°C in 20 mM HEPES/KOH (pH 7.4), 100 mM KCl, 5 mM $MgCl_2$, and 5% glycerol. Cysteine variants were labeled with Atto532 maleimide (donor, Atto-Tec, GmbH; Siegen, Germany) and Atto647N maleimide (acceptor, Atto-Tec, GmbH) as described in Supplemental Experimental Procedures.

Cysteine variants of DnaK were purified and labeled as described for Ssc1. Essentially the same results were obtained if Ssc1 and DnaK variants were expressed in BL21(DE3) Δ*dnaK*::52 cells (a gift of B. Bukau and M. Mayer, ZMBH; Heidelberg, Germany). Mdj1 and Mge1 were purified as described previously (Horst et al., 1997) and labeled as described in Supplemental Experimental Procedures.

Steady-State and Kinetic Ensemble FRET Measurements

Steady-state and kinetic ensemble FRET measurements were performed at 25°C on Fluorolog-3 spectrofluorometer (HORIBA Jobin Yvon GmbH; Unterhaching, Germany) using Atto532 as donor and Atto647N as acceptor fluorophores, unless otherwise indicated. Kinetic measurements under stopped-flow conditions were performed on Applied Photophysics SX.18MV with a 1:1 mixing ratio at 25°C. Kinetic traces shown are averages of 10–12 independent measurements. Details are given in Supplemental Experimental Procedures.

Single-Pair FRET Experiments

SpFRET measurements were performed on dual-color confocal systems using PIE (Müller et al., 2005) with polarization-sensitive detection for multiparameter fluorescence detection. The double-labeled proteins were diluted in the buffer used for ensemble measurements to a concentration of ~20–40 pM to ensure that the probability of having two or more particles in the probe volume at the same time is negligible (<1%). For an individual experiment, at least 500 particles were measured, and the experiments were repeated with different protein preparations to verify the reproducibility of the results. Details are provided in Supplemental Experimental Procedures.

SUPPLEMENTAL INFORMATION

Supplemental Information includes Supplemental Experimental Procedures, Supplemental References, four tables, and three figures and can be found with this article online at doi:10.1016/j.molcel.2010.03.010.

ACKNOWLEDGMENTS

We wish to thank M. Hayer-Hartl and F.U. Hartl for use of their stopped-flow equipment; K. Chakraborty, Z. Dragovic, and C. Bräuchle for fruitful discussions; and P. Robisch and M. Malesic for expert technical assistance. We gratefully acknowledge the financial support of the Deutsche Forschungsgemeinschaft (SFB 594 to D.M. and W.N. and SFB 749 to D.C.L.), the German-Israeli Foundation, the Ludwig-Maximilians-University Munich (LMUInnovativ BioImaging Network), and Nanosystems Initiative Munich (NIM).

Received: June 7, 2009
Revised: February 3, 2010
Accepted: March 22, 2010
Published: April 8, 2010

REFERENCES

Andréasson, C., Fiaux, J., Rampelt, H., Druffel-Augustin, S., and Bukau, B. (2008). Insights into the structural dynamics of the Hsp110-Hsp70 interaction reveal the mechanism for nucleotide exchange activity. Proc. Natl. Acad. Sci. USA *105*, 16519–16524.

Antonik, M., Felekyan, S., Gaiduk, A., and Seidel, C.A. (2006). Separating structural heterogeneities from stochastic variations in fluorescence resonance energy transfer distributions via photon distribution analysis. J. Phys. Chem. B *110*, 6970–6978.

Baumann, F., Milisav, I., Neupert, W., and Herrmann, J.M. (2000). Ecm10, a novel hsp70 homolog in the mitochondrial matrix of the yeast Saccharomyces cerevisiae. FEBS Lett. *487*, 307–312.

Bertelsen, E.B., Chang, L., Gestwicki, J.E., and Zuiderweg, E.R. (2009). Solution conformation of wild-type E. coli Hsp70 (DnaK) chaperone complexed with ADP and substrate. Proc. Natl. Acad. Sci. USA *106*, 8471–8476.

Bhattacharya, A., Kurochkin, A.V., Yip, G.N.B., Zhang, Y., Bertelsen, E.B., and Zuiderweg, E.R. (2009). Allostery in Hsp70 chaperones is transduced by subdomain rotations. J. Mol. Biol. *388*, 475–490.

Bolender, N., Sickmann, A., Wagner, R., Meisinger, C., and Pfanner, N. (2008). Multiple pathways for sorting mitochondrial precursor proteins. EMBO Rep. *9*, 42–49.

Brodsky, J.L. (1996). Post-translational protein translocation: not all hsc70s are created equal. Trends Biochem. Sci. *21*, 122–126.

Buchberger, A., Theyssen, H., Schröder, H., McCarty, J.S., Virgallita, G., Milkereit, P., Reinstein, J., and Bukau, B. (1995). Nucleotide-induced conformational changes in the ATPase and substrate binding domains of the DnaK chaperone provide evidence for interdomain communication. J. Biol. Chem. *270*, 16903–16910.

Bukau, B., and Horwich, A.L. (1998). The Hsp70 and Hsp60 chaperone machines. Cell *92*, 351–366.

Bukau, B., Weissman, J., and Horwich, A. (2006). Molecular chaperones and protein quality control. Cell *125*, 443–451.

Chang, Y.W., Sun, Y.J., Wang, C., and Hsiao, C.D. (2008). Crystal structures of the 70-kDa heat shock proteins in domain disjoining conformation. J. Biol. Chem. *283*, 15502–15511.

Craig, E.A., and Marszalek, J. (2002). A specialized mitochondrial molecular chaperone system: a role in formation of Fe/S centers. Cell. Mol. Life Sci. *59*, 1658–1665.

Craig, E.A., Kramer, J., and Kosic-Smithers, J. (1987). SSC1, a member of the 70-kDa heat shock protein multigene family of Saccharomyces cerevisiae, is essential for growth. Proc. Natl. Acad. Sci. USA *84*, 4156–4160.

Craig, E.A., Huang, P., Aron, R., and Andrew, A. (2006). The diverse roles of J-proteins, the obligate Hsp70 co-chaperone. Rev. Physiol. Biochem. Pharmacol. *156*, 1–21.

Deloche, O., Kelley, W.L., and Georgopoulos, C. (1997). Structure-function analyses of the Ssc1p, Mdj1p, and Mge1p Saccharomyces cerevisiae mitochondrial proteins in Escherichia coli. J. Bacteriol. *179*, 6066–6075.

Deocaris, C.C., Kaul, S.C., and Wadhwa, R. (2009). The versatile stress protein mortalin as a chaperone therapeutic agent. Protein Pept. Lett. *16*, 517–529.

Endo, T., Yamamoto, H., and Esaki, M. (2003). Functional cooperation and separation of translocators in protein import into mitochondria, the double-membrane bounded organelles. J. Cell Sci. *116*, 3259–3267.

Frydman, J. (2001). Folding of newly translated proteins in vivo: the role of molecular chaperones. Annu. Rev. Biochem. *70*, 603–647.

Gansen, A., Valeri, A., Hauger, F., Felekyan, S., Kalinin, S., Tóth, K., Langowski, J., and Seidel, C.A. (2009). Nucleosome disassembly intermediates characterized by single-molecule FRET. Proc. Natl. Acad. Sci. USA *106*, 15308–15313.

Genevaux, P., Georgopoulos, C., and Kelley, W.L. (2007). The Hsp70 chaperone machines of Escherichia coli: a paradigm for the repartition of chaperone functions. Mol. Microbiol. *66*, 840–857.

Hennessy, F., Nicoll, W.S., Zimmermann, R., Cheetham, M.E., and Blatch, G.L. (2005). Not all J domains are created equal: implications for the specificity of Hsp40-Hsp70 interactions. Protein Sci. *14*, 1697–1709.

Horst, M., Oppliger, W., Rospert, S., Schönfeld, H.J., Schatz, G., and Azem, A. (1997). Sequential action of two hsp70 complexes during protein import into mitochondria. EMBO J. *16*, 1842–1849.

Jiang, J., Prasad, K., Lafer, E.M., and Sousa, R. (2005). Structural basis of interdomain communication in the Hsc70 chaperone. Mol. Cell *20*, 513–524.

Jiang, J., Maes, E.G., Taylor, A.B., Wang, L., Hinck, A.P., Lafer, E.M., and Sousa, R. (2007). Structural basis of J cochaperone binding and regulation of Hsp70. Mol. Cell *28*, 422–433.

Kalinin, S., Felekyan, S., Antonik, M., and Seidel, C.A. (2007). Probability distribution analysis of single-molecule fluorescence anisotropy and resonance energy transfer. J. Phys. Chem. B *111*, 10253–10262.

Kalinin, S., Felekyan, S., Valeri, A., and Seidel, C.A. (2008). Characterizing multiple molecular States in single-molecule multiparameter fluorescence detection by probability distribution analysis. J. Phys. Chem. B *112*, 8361–8374.

Kang, P.J., Ostermann, J., Shilling, J., Neupert, W., Craig, E.A., and Pfanner, N. (1990). Requirement for hsp70 in the mitochondrial matrix for translocation and folding of precursor proteins. Nature *348*, 137–143.

Kapanidis, A.N., Lee, N.K., Laurence, T.A., Doose, S., Margeat, E., and Weiss, S. (2004). Fluorescence-aided molecule sorting: analysis of structure and interactions by alternating-laser excitation of single molecules. Proc. Natl. Acad. Sci. USA *101*, 8936–8941.

Koehler, C.M. (2004). New developments in mitochondrial assembly. Annu. Rev. Cell Dev. Biol. *20*, 309–335.

Lisse, T., and Schwarz, E. (2000). Functional specificity of the mitochondrial DnaJ protein, Mdj1p, in Saccharomyces cerevisiae. Mol. Gen. Genet. *263*, 527–534.

Liu, Q., and Hendrickson, W.A. (2007). Insights into Hsp70 chaperone activity from a crystal structure of the yeast Hsp110 Sse1. Cell *131*, 106–120.

Mayer, M.P., and Bukau, B. (2005). Hsp70 chaperones: cellular functions and molecular mechanism. Cell. Mol. Life Sci. *62*, 670–684.

Misselwitz, B., Staeck, O., Matlack, K.E., and Rapoport, T.A. (1999). Interaction of BiP with the J-domain of the Sec63p component of the endoplasmic reticulum protein translocation complex. J. Biol. Chem. *274*, 20110–20115.

Mokranjac, D., Bourenkov, G., Hell, K., Neupert, W., and Groll, M. (2006). Structure and function of Tim14 and Tim16, the J and J-like components of the mitochondrial protein import motor. EMBO J. *25*, 4675–4685.

Moro, F., Okamoto, K., Donzeau, M., Neupert, W., and Brunner, M. (2002). Mitochondrial protein import: molecular basis of the ATP-dependent interaction of MtHsp70 with Tim44. J. Biol. Chem. *277*, 6874–6880.

Müller, B.K., Zaychikov, E., Bräuchle, C., and Lamb, D.C. (2005). Pulsed interleaved excitation. Biophys. J. *89*, 3508–3522.

Neupert, W., and Brunner, M. (2002). The protein import motor of mitochondria. Nat. Rev. Mol. Cell Biol. *3*, 555–565.

Neupert, W., and Herrmann, J.M. (2007). Translocation of proteins into mitochondria. Annu. Rev. Biochem. *76*, 723–749.

Polier, S., Dragovic, Z., Hartl, F.U., and Bracher, A. (2008). Structural basis for the cooperation of Hsp70 and Hsp110 chaperones in protein folding. Cell *133*, 1068–1079.

Rehling, P., Brandner, K., and Pfanner, N. (2004). Mitochondrial import and the twin-pore translocase. Nat. Rev. Mol. Cell Biol. *5*, 519–530.

Rowley, N., Prip-Buus, C., Westermann, B., Brown, C., Schwarz, E., Barrell, B., and Neupert, W. (1994). Mdj1p, a novel chaperone of the DnaJ family, is involved in mitochondrial biogenesis and protein folding. Cell *77*, 249–259.

Saibil, H.R. (2008). Chaperone machines in action. Curr. Opin. Struct. Biol. *18*, 35–42.

Schilke, B., Williams, B., Knieszner, H., Pukszta, S., D'Silva, P., Craig, E.A., and Marszalek, J. (2006). Evolution of mitochondrial chaperones utilized in Fe-S cluster biogenesis. Curr. Biol. *16*, 1660–1665.

Schuermann, J.P., Jiang, J., Cuellar, J., Llorca, O., Wang, L., Gimenez, L.E., Jin, S., Taylor, A.B., Demeler, B., Morano, K.A., et al. (2008). Structure of the Hsp110:Hsc70 nucleotide exchange machine. Mol. Cell *31*, 232–243.

Sharma, S., Chakraborty, K., Müller, B.K., Astola, N., Tang, Y.C., Lamb, D.C., Hayer-Hartl, M., and Hartl, F.U. (2008). Monitoring protein conformation along the pathway of chaperonin-assisted folding. Cell *133*, 142–153.

Sichting, M., Mokranjac, D., Azem, A., Neupert, W., and Hell, K. (2005). Maintenance of structure and function of mitochondrial Hsp70 chaperones requires the chaperone Hep1. EMBO J. *24*, 1046–1056.

Swain, J.F., Schulz, E.G., and Gierasch, L.M. (2006). Direct comparison of a stable isolated Hsp70 substrate-binding domain in the empty and substrate-bound states. J. Biol. Chem. *281*, 1605–1611.

Swain, J.F., Dinler, G., Sivendran, R., Montgomery, D.L., Stotz, M., and Gierasch, L.M. (2007). Hsp70 chaperone ligands control domain association via an allosteric mechanism mediated by the interdomain linker. Mol. Cell *26*, 27–39.

Vogel, M., Bukau, B., and Mayer, M.P. (2006a). Allosteric regulation of Hsp70 chaperones by a proline switch. Mol. Cell *21*, 359–367.

Vogel, M., Mayer, M.P., and Bukau, B. (2006b). Allosteric regulation of Hsp70 chaperones involves a conserved interdomain linker. J. Biol. Chem. *281*, 38705–38711.

Voos, W., and Röttgers, K. (2002). Molecular chaperones as essential mediators of mitochondrial biogenesis. Biochim. Biophys. Acta *1592*, 51–62.

Walsh, P., Bursać, D., Law, Y.C., Cyr, D., and Lithgow, T. (2004). The J-protein family: modulating protein assembly, disassembly and translocation. EMBO Rep. *5*, 567–571.

Weiss, C., Niv, A., and Azem, A. (2002). Two-step purification of mitochondrial Hsp70, Ssc1p, using Mge1(His)(6) immobilized on Ni-agarose. Protein Expr. Purif. *24*, 268–273.

Westermann, B., Gaume, B., Herrmann, J.M., Neupert, W., and Schwarz, E. (1996). Role of the mitochondrial DnaJ homolog Mdj1p as a chaperone for mitochondrially synthesized and imported proteins. Mol. Cell. Biol. *16*, 7063–7071.

Woo, H.-J., Jiang, J., Lafer, E.M., and Sousa, R. (2009). ATP-induced conformational changes in Hsp70: molecular dynamics and experimental validation of an in silico predicted conformation. Biochemistry *48*, 11470–11477.

Yoneda, T., Benedetti, C., Urano, F., Clark, S.G., Harding, H.P., and Ron, D. (2004). Compartment-specific perturbation of protein handling activates genes encoding mitochondrial chaperones. J. Cell Sci. *117*, 4055–4066.

Young, J.C., Agashe, V.R., Siegers, K., and Hartl, F.U. (2004). Pathways of chaperone-mediated protein folding in the cytosol. Nat. Rev. Mol. Cell Biol. *5*, 781–791.

Zhu, X., Zhao, X., Burkholder, W.F., Gragerov, A., Ogata, C.M., Gottesman, M.E., and Hendrickson, W.A. (1996). Structural analysis of substrate binding by the molecular chaperone DnaK. Science *272*, 1606–1614.